Available online at www.sciencedirect.com
ScienceDirect
Trans. Nonferrous Met. Soc. China 25(2015) 1206−1214
Transactions of Nonferrous Metals Society of China
www.tnmsc.cn

Microstructure and properties of rare earth-containing Cu−Cr−Zr alloy

Zhen-ya PAN, Jiang-biao CHEN, Jin-fu LI

State Key Laboratory of Metal Matrix Composites, School of Materials Science and Engineering, Shanghai Jiao Tong University, Shanghai 200240, China

Received 13 April 2014; accepted 7 August 2014

Abstract: Cu−0.81Cr−0.12Zr−0.05La−0.05Y (mass fraction) alloy was successively subjected to hot rolling, solid solution treatment, cold rolling and aging treatments. Its microstructure, microhardness and electrical conductivity at different states were systematically investigated. The as-cast microstructure consists of three phases: Cu matrix, Cr and Cu_5Zr. Zr is completely dissolved into the matrix while partial Cr remains after the solid solution treatment. Aging of the cold-rolled sample makes nanocrystals of Cr and Cu_5Zr precipitate from the matrix, and the microhardness and electrical conductivity rise. A combination of high microhardness (HV 186) and high conductivity (81% IACS) can be obtained by aging the sample at 773 K for 60 min. As the aging temperature increases, the orientation degree of the Cu crystals gradually decreases to zero, but the microstrain in them cannot be eliminated completely owing to the presence of precipitates and dislocations. The Cr precipitates exhibit the N−W orientation relationship with the matrix when the coherence strengthening mechanism plays a main role.

Key words: Cu−Cr−Zr−RE alloy; rolling; aging treatment; microstructure; properties

1 Introduction

The solubilities of Cr and Zr in Cu are very low at room temperature. When the Cr- and Zr-supersaturated copper alloys are aged at medium temperatures, these two alloying elements precipitate from the matrix as single-component phases or intermetallic compounds. The fine precipitates dispersing in the matrix make a great contribution to the strength without doing harm to the electrical conductivity. Cu−Cr−Zr alloys are therefore widely used in fabrication of the components requiring high mechanical strength and good electrical conductivity, such as integrated circuit lead frames, electronic connectors, and resistance welding electrodes [1−4].

To achieve a better combination of strength and conductivity properties, tremendous efforts have been made in the alloy composition design and the processing technology improvement. SU et al [5] rapidly solidified Cu−0.36Cr−0.23Sn−0.15Zn alloy and aged the sample between 673 and 873 K. The hardness was increased up to HV 178, while the electrical conductivity was still maintained above 60.6% IACS. MU et al [6] added Mg and rare earth (Ce or La) to the copper alloy, and applied an additional cold rolling operation before aging. As a result, a microhardness as high as HV 118 and an electrical conductivity high up to 82% IACS were achieved.

Rare earths (RE) belong to the most reactive metals, and almost cannot be dissolved into copper at room temperature. They form compounds with other alloy elements and play an important part in decontamination of the alloy melt. It is also believed that addition of RE can reduce the electron scattering probability in the copper alloys and therefore increase the conductivity to a certain degree [7,8]. However, the work to date was focused on the role of single rare earth element, and the knowledge about the effect of misch metal is very limited. In this study, a Cu−Cr−Zr alloy containing La and Y was synthesized. Its microstructure and properties at different processing stages were investigated. It is revealed that the simultaneous addition of Y and La is more favorable for improving the performance of the Cu−Cr−Zr alloy.

2 Experimental

Cu−0.81Cr−0.12Zr−0.05La−0.05Y (mass fraction) alloy ingots were produced by induction melting pure

Foundation item: Project (51227001) supported by the National Natural Science Foundation of China; Project (2011CB610405) supported by the National Basic Research Program of China
Corresponding author: Jin-fu LI; Tel/Fax: +86-21-54748530; E-mail: jfli@sjtu.edu.cn
DOI: 10.1016/S1003-6326(15)63717-7

copper (99.99%), chromium (99.999%), zirconium (99.9%), lanthanum (99.5%) and yttrium (99.8%) in a vacuum furnace under the protection of high purity argon. To prevent Zr from reacting with the crucible, Zr lumps were added at last. The as-cast ingots were homogenized at 1193 K for 120 min and then hot-rolled into sheets of 5 mm in thickness. After solid solution was treated at 1223 K for 60 min, the sheets were quenched into water. Subsequently, the sheets were cold-rolled to 2 mm in thickness and cut into small pieces (100 mm × 10 mm× 2 mm) for the aging treatment in a vacuum annealing furnace. The aging temperature and time ranged from 673 to 873 K and 15 to 360 min, respectively, and the temperature accuracy was controlled within ±1 K.

Microhardness was measured in an HVS−1000 type hardness tester under a load of 100 g and holding time of 20 s. Each sample was tested five times. Electrical resistance was measured with the sample of 40 mm in length by the four–probe method. The precipitation kinetics from room temperature to 873 K was analyzed by a differential scanning calorimeter (DSC, Perkin-Elmer Pyris Diamond type) at a heating rate of 20 K/min. The phase constitution was analyzed using a Thermo ARL X-ray diffractometer (XRD) with monochromatic Cu K_α radiation (λ=0.154 nm). The microstrain was calculated by analysis of the XRD peak broadening. The microstructures of various samples were observed by a JSM−7600 scanning electron microscope (SEM) equipped with energy dispersive X-ray spectroscope (EDXS). The precipitated phase was identified by a JEM2100F high resolution transmission electron microscope (HRTEM). The HRTEM foils of 3 mm in diameter were cut from the aged sample. They were ground to 60−90 μm in thickness, and then thinned by twin-jet polishing in a solution of $V(HNO_3)$:$V(CH_2OH)$= 1:9 at about 243 K. The operating voltage for HRTEM observation was 300 kV.

3 Results and discussion

3.1 Microstructure evolution

Figure 1 shows the backscattered electron images of

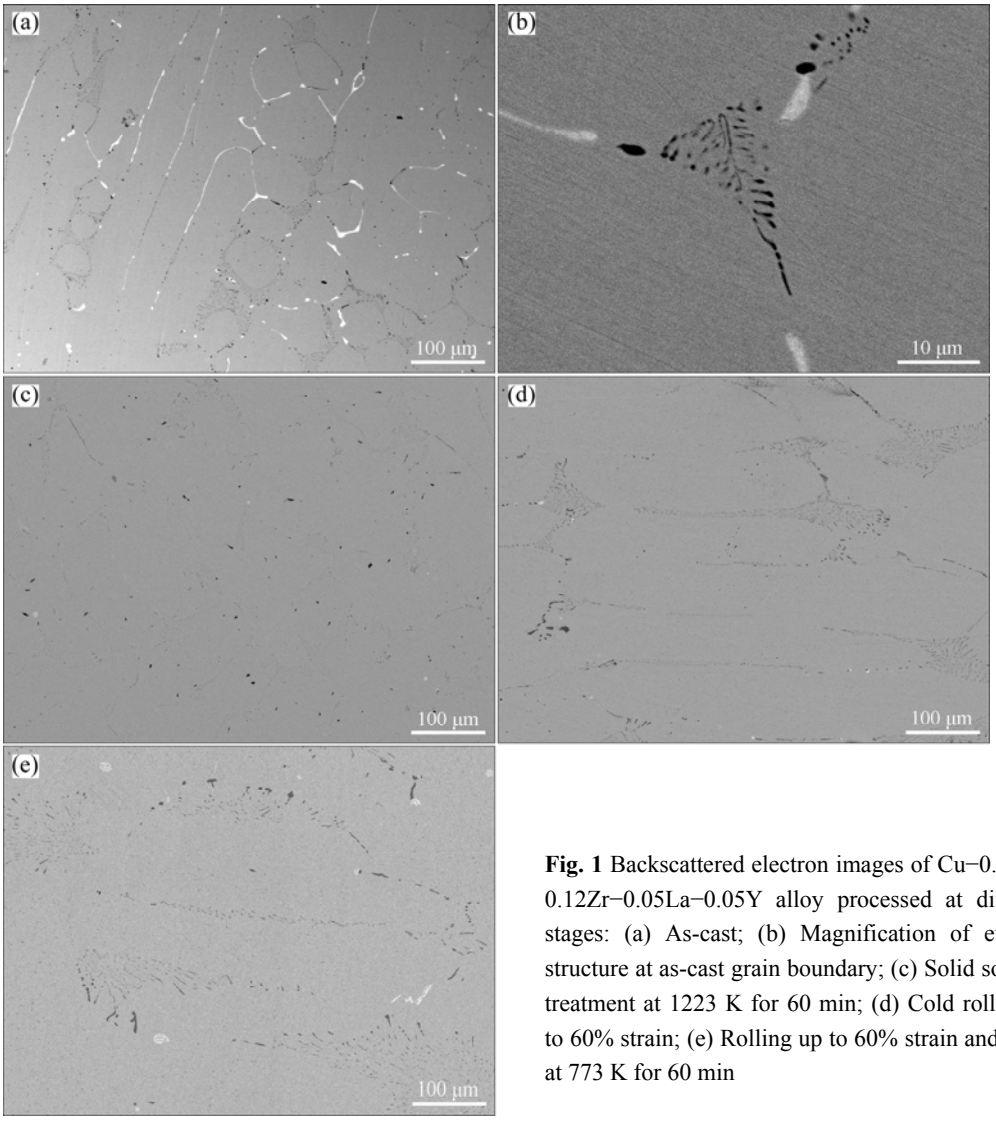

Fig. 1 Backscattered electron images of Cu−0.81Cr−0.12Zr−0.05La−0.05Y alloy processed at different stages: (a) As-cast; (b) Magnification of eutectic structure at as-cast grain boundary; (c) Solid solution treatment at 1223 K for 60 min; (d) Cold rolling up to 60% strain; (e) Rolling up to 60% strain and aging at 773 K for 60 min

the Cu−0.81Cr−0.12Zr−0.05La−0.05Y alloy processed at different stages. From Fig. 1(a), it can be seen that there are lots of bright and dark particles distributing at the grain boundaries of the alloy ingots. The particles inside the grains are very few. When the microstructure was observed at a larger magnification, eutectic structures at the triangular boundaries are revealed (Fig. 1(b)). Compared with the microstructure of Cu−0.81Cr−0.12Zr alloy [9], it is known that the misch metals added to the Cu−Cr−Zr alloy act as a grain refiner, resulting in fine and uniform microstructure in the present alloy.

The results of identifying the phases in the alloy ingot by EDXS are shown in Fig. 2 and Table 1. The dark phase at the grain boundary contains about 83.75% Cr and 16.25% Cu (mole fraction, the same below if not mentioned). Considering that the solid solubility of Cr in Cu is very small at room temperature and Cr cannot form compounds with Cu, the dark phase should be pure Cr. In this case, The Cu signal in the EDXS spectrum should result from the Cu matrix. The bright phase contains about 78.66% Cu, 14.19% Zr, 4.25% Y and 2.90% La. The mole ratio of Cu to Zr atoms is 5.54:1, indicating that the phase should be Cu_5Zr doped with Y and La.

The crystal grains became equiaxed after the solid solution treatment at 1223 K for 60 min, as shown in Fig. 1(c), where most of solutes Cr and Zr have been dissolved in the Cu matrix except several large Cr particles survived. Figures 1(d) and (e) show the microstructure of the sample cold-rolled up to 60% strain and that further aged at 773 K for 60 min, within which elongated grains along the rolling direction can be observed.

Figure 3 shows the DSC curve when the cold-rolled sample was heated from room temperature at a rate of 20 K/min. Exothermic reactions associated with annihilation of crystal defects and coarsening of grains take place in the annealing process, leading to a concave curve. The small sharp exothermic peak with an onset temperature of 653 K and an end temperature of 698 K results from the precipitation reaction. The microstructure of the sample heated up to 698 K in the DSC is shown in Fig. 4(a), from which it can be known that Cr and Cu_5Zr phases have precipitated again. The second exothermal peak that starts from 743 K, and ends at 823 K is associated with recrystallization, during which the Cr and Cu_5Zr particles are coarsened while the grains of the Cu matrix become equiaxed (Fig. 4(b)).

3.2 Properties

After solid solution treatment, cold-rolling prior to aging has been verified to be an effective strengthening method to elevate the comprehensive performance of Cu−Cr−Zr alloys [6]. The reason is that the induced high density of point defects and severe lattice distortion provide more nucleation sites, and correspondingly

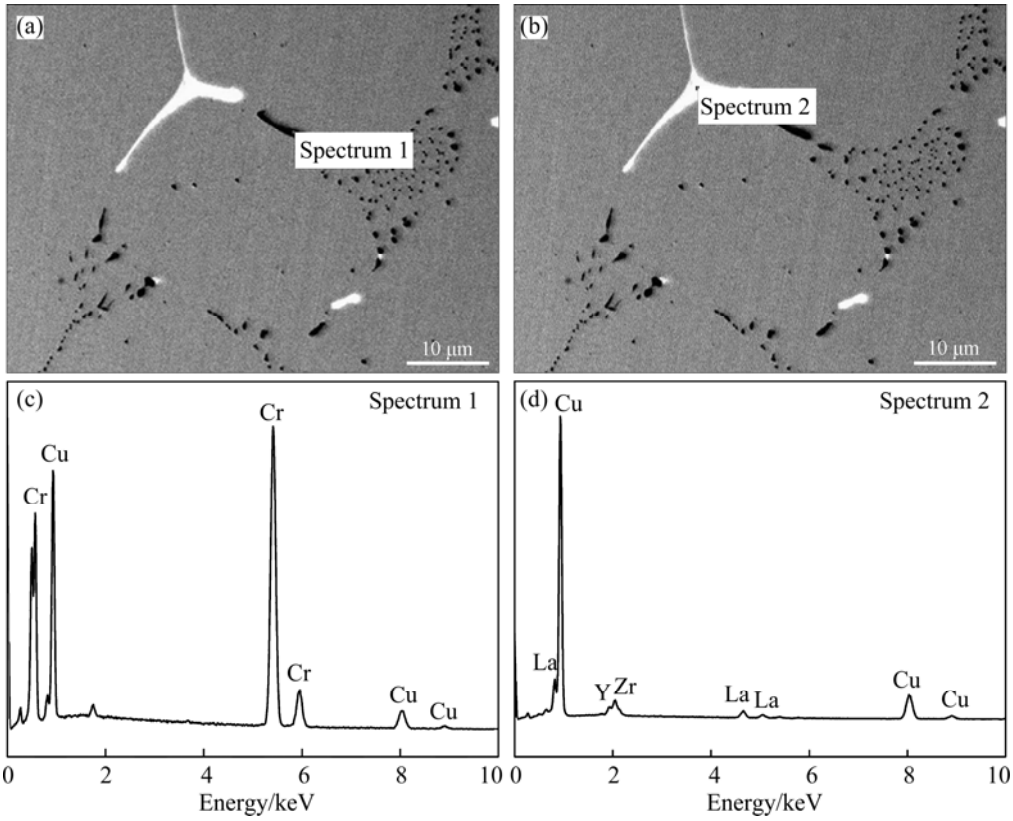

Fig. 2 Morphologies of dark (a) and bright (b) phases at grain boundary of alloy ingot and corresponding EDXS spectra of (c, d)

Table 1 EDXS analysis results of dark and bright phases in Fig. 2

Phase	Mole fraction/%					
	Cu	Cr	Zr	Y	La	Total
Dark phase	16.25	83.75	0	0	0	100
Bright phase	78.66	0	14.19	4.25	2.90	100

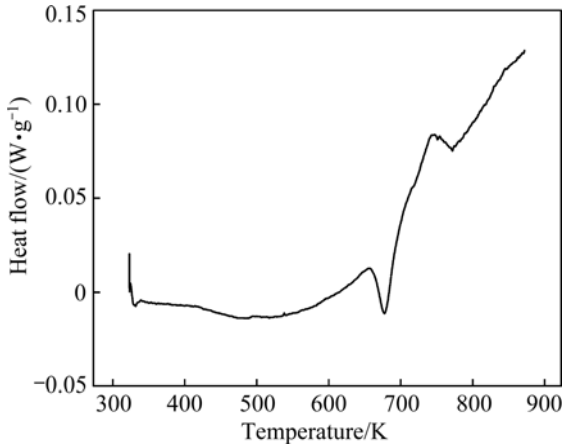

Fig. 3 DSC curve of Cu−0.81Cr−0.12Zr−0.05La−0.05Y specimen cold-rolled up to 60% strain and heated at rate of 20 K/min

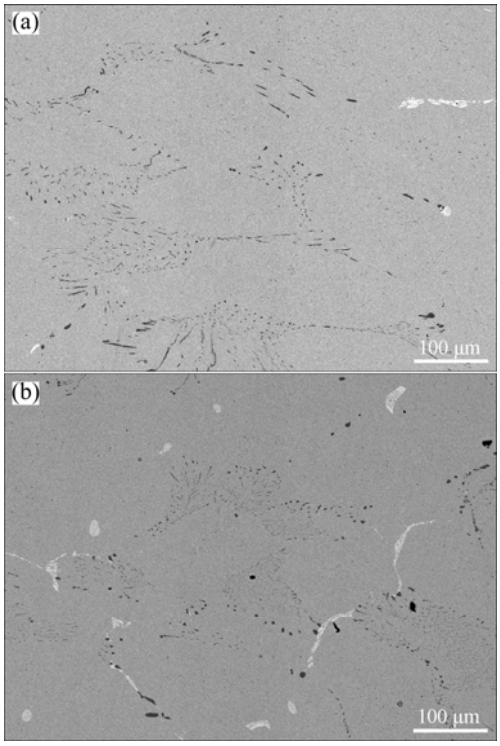

Fig. 4 Microstructures of Cu−0.81Cr−0.12Zr−0.05La−0.05Y specimen cold rolled up to 60% strain and heated to 698 K (a) and 823 K (b) at 20 K/min

refine the precipitated phases during the aging treatment [10,11].

Figure 5 shows the microhardness and electrical conductivity variations when the Cu−0.81Cr−0.12Zr−0.05La−0.05Y alloy cold-rolled up to 60% strain is aged below the onset temperature of recrystallization. At the aging temperature of 673 K, the microhardness increases first quickly and then slowly with increasing the aging time. As the aging temperature is raised to 723 K, the microhardness increases more quickly at the initial stage of aging, but then decreases, namely overaging occurs. At the aging temperature of 773 K, the microhardness gets to the maximum HV 186 after the specimen was aged for 60 min. The peak hardness decreases if the aging temperature is further increased. The higher the aging temperature is, the faster the solute diffusion speed and therefore the shorter the time to reach the microhardness peak will be. In the present experiment, a Cu−0.81Cr−0.12Zr−0.05La−0.05Y alloy ingot was ever reheated near the solubility limit line, and then quenched into water. After it was aged at 773 K for 60 min, the microhardness was measured to be only HV 125. Obviously, the additional cold-rolling process has evidently enhanced the aging precipitation hardening, as found in other alloys [12].

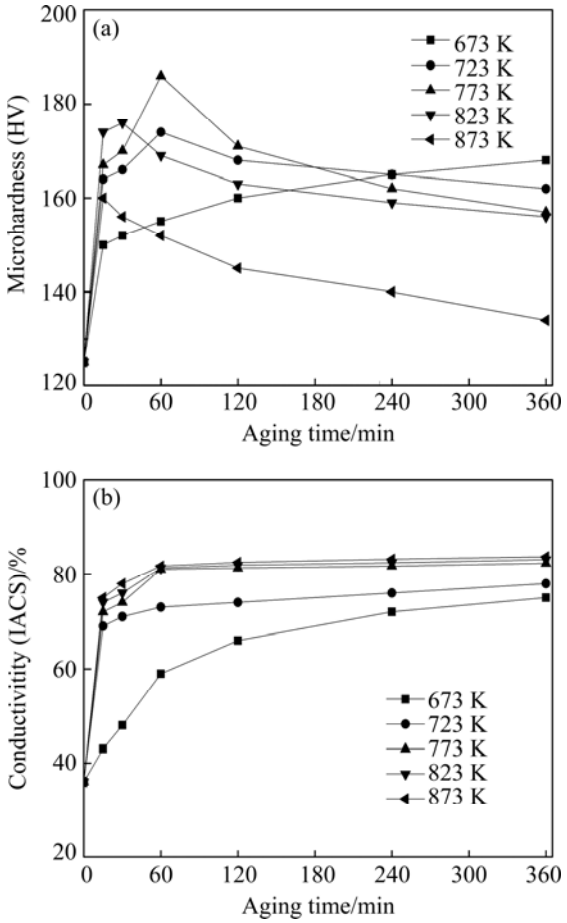

Fig. 5 Microhardness (a) and electrical conductivity (b) changes of Cu−0.81Cr−0.12Zr−0.05La−0.05Y alloy cold-rolled up to 60% strain and aged at various temperatures

The electrical conductivity of the cold-rolled sample is very low, being only 36% IACS. The reason is that

excessive solute atoms were supersaturated in the copper matrix after solution treatment, and a high density of dislocations was introduced by cold-rolling processing. They act as obstacles to the movement of electrons and increase the probability of electron scattering [13]. As the supersaturated solute atoms precipitated from the matrix and the distorted lattice recovered in the aging, the electrical conductivity increased quickly at the initial stage. The slope of the curve becomes steeper at higher aging temperatures as a result of the accelerated kinetics of precipitation.

Different from microhardness, electrical conductivity does not decrease after the initial rapid rise. The raising of aging temperature results in a larger conductivity. For example, aging the sample at 673 K for 60 min affords a conductivity of 59% IACS, while aging at 873 K for 60 min increases the conductivity to 81.7% IACS. Although overaging occurs as the aging temperature exceeds 773 K, the growth of the precipitates does little harm to the electrical conductivity of the alloy.

A good combination of mechanical and electrical properties is obtained in the Cu−0.81Cr−0.12Zr−0.05La−0.05Y alloy aged at 773 K for 60 min. Its microhardness reaches HV 186 and the electrical conductivity is 81% IACS.

Besides Cu−0.81Cr−0.12Zr−0.05La−0.05Y alloy, Cu−0.81Cr−0.12Zr, Cu−0.81Cr−0.12Zr−0.05Y and Cu−0.81Cr−0.12Zr−0.05La alloys were also prepared and processed following the same procedure. The properties of all the alloys aged at 773 K for 30 and 60 min respectively are listed in Table 2. It is clear that the separate addition of Y or La increases the microhardness but decreases the electrical conductivity. Simultaneous addition of La and Y gets the largest rise in microhardness while the decrease in electrical conductivity is the lowest.

Table 2 Properties of alloys cold-rolled up to 60% strain and aged at 773 K for 30 and 60 min, respectively

Alloy	Microhardness (HV)		Electrical conductivity (IACS)/%	
	30 min	60 min	30 min	60 min
Cu−0.81Cr−0.12Zr	161	174	76	82
Cu−0.81Cr−0.12Zr−0.05Y	164	179	73	80.5
Cu−0.81Cr−0.12Zr−0.05La	166	181	72	80
Cu−0.81Cr−0.12Zr−0.05La−0.05Y	170	186	74	81

3.3 Orientation and microstrain

Both mechanical and electrical properties of the precipitation strengthening Cu alloys are sensitive to the aging parameters. Figure 6 shows the XRD patterns of the Cu−0.81Cr−0.12Zr−0.05La−0.05Y alloy that was cold-rolled by 60% strain and aged for 60 min at various temperatures.

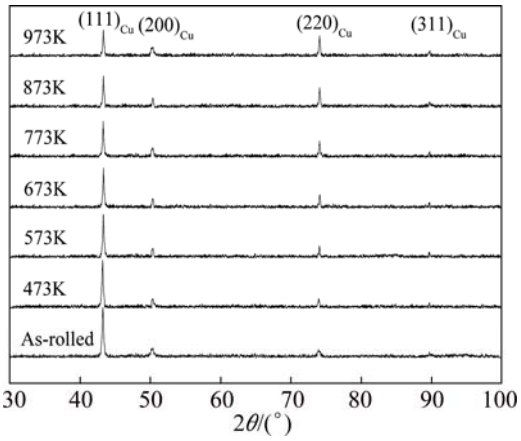

Fig. 6 XRD patterns of Cu−0.81Cr−0.12Zr−0.05La−0.05Y alloy cold-rolled by 60% strain and then aged at various temperatures for 60 min

Although there is only the diffraction peak of Cu to be detected in all the specimens, a clear change can be found in the peak intensity. For example, the $(111)_{Cu}$ intensity is the highest in the as-rolled specimen and decreases with the increasing aging temperature. In contrast with the $(111)_{Cu}$ peak, the $(220)_{Cu}$ intensity exhibits a reverse change. It is the lowest in the as-rolled specimens but increases with the increasing aging temperature. These indicate that the aging treatment has changed the crystal orientation in the as-rolled alloy.

The degree of crystal orientation can be expressed by the Lotgering factors [14]:

$$L_{(hkl)} = (P_{(hkl)} - P'_{(hkl)})/(1 - P'_{(hkl)}) \quad (1)$$

$$P_{(hkl)} = I_{(hkl)})/\sum_i I_j \quad (2)$$

$$P'_{(hkl)} = I'_{(hkl)})/\sum_i I'_j \quad (3)$$

where $I_{(hkl)}$ and $I'_{(hkl)}$ are the (*hkl*) diffraction intensities in the as-rolled specimen and fully annealed specimen, respectively, and I_j and I'_j are the any diffraction intensities in the as-rolled specimens and fully annealed specimen respectively. $I'_{(hkl)}$ and I'_j can be determined from the XRD pattern of the specimen aged at 973 K, where the microstructure was replaced by equiaxed grains completely. The $L_{(hkl)}$ calculated from the XRD patterns shown in Fig. 6 is illustrated in Fig. 7(a). With increasing the aging temperature, the degree of crystal orientation decreases and gets to zero at the aging temperature of 973 K.

Figure 7(b) shows the microstrain of specimen from the XRD patterns aged at different temperatures for

60 min. As the aging temperature increases below 573 K, the microstrain decreases slowly because only a small portion of the stored energy is released and the internal stress relaxed by the recovery is very limited. When the aging temperature increases above 573 K, the microstrain decreases quickly because the stored energy is released efficiently due to the recovery and the recrystallization process. In recent years, extensive literatures have been available on the microstrain in pure Cu. The microstrain was determined to be 0.16% in the cold-rolled Cu [15], 0.24% in the magnetron sputtered Cu [16] and 0.1% in the equal-channel angular pressed Cu [17]. By comparison, the microstrain in the cold-rolled Cu−0.81Cr−0.12Zr−0.05La−0.05Y alloy is larger because of the interaction of precipitates and dislocations [18,19].

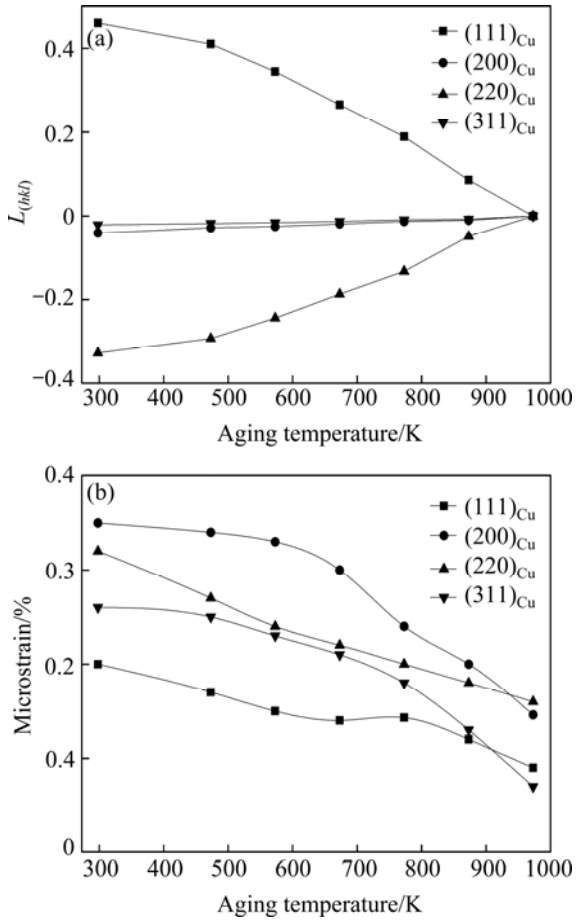

Fig. 7 Lotgering factor (a) and microstrain (b) derived from XRD patterns shown in Fig. 6

3.4 Coherent relationship between precipitates and matrix

Figure 8 shows the TEM and HRTEM images of the alloy cold-rolled by 60% strain and aged at 773 K for 60 min. It can be seen that small and well-dispersed particles precipitate from the matrix that still has a high density of dislocations including pile-up of dislocations and dislocation tangle (Fig. 8(a)). The spherical precipitates of about 5 nm in diameter have a coherent or semicoherent relationship with the copper matrix, indicated by the fact that the lattice fringes of one phase stretch into another phase, namely, the crystal lattices on both side converge at the boundary, and the boundary atoms are shared by the matrix and precipitate (Fig. 8(b)).

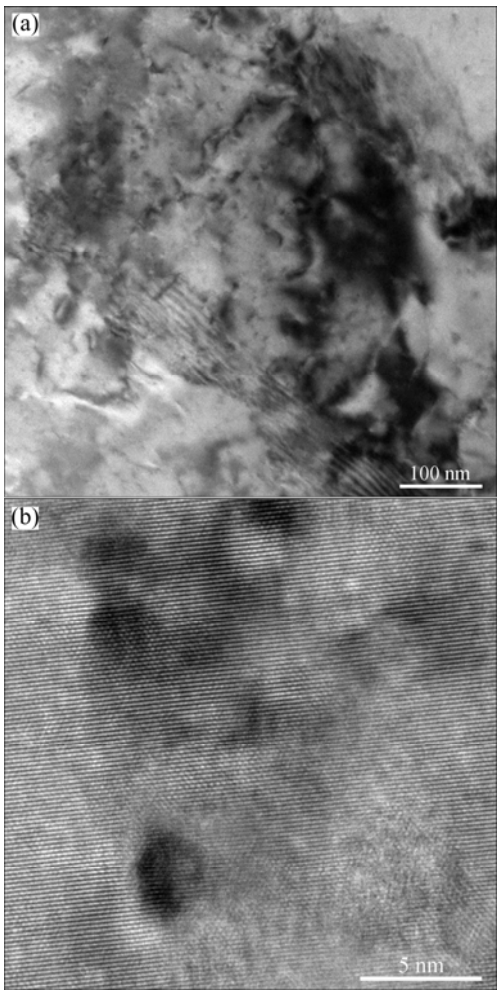

Fig. 8 TEM (a) and HRTEM (b) bright field images of Cu−0.81Cr−0.12Zr−0.05La−0.05Y specimen cold-rolled by 60% strain and aged at 773 K for 60 min

Mechanical and electronic properties of copper alloys depend on the size and distribution of the precipitates. For comparison, Fig. 9 shows the TEM images and selected area electron diffraction (SAED) patterns of the specimens cold-rolled up to 60% strain and aged at 723 K and 773 K respectively for 60 min to the microhardness peak and that overaged at 823 K for 60 min. The spherical precipitates homogeneously dispersed in the matrix are about 2−5 nm and 5−10 nm in diameter, respectively, when the aging temperatures are 723 K (Fig. 9(a)) and 773 K (Fig. 9(c)). The peak microhardness of the specimen aged at 773 K is higher than that aged at 723 K because more precipitates form, which hinders the movement of dislocations more

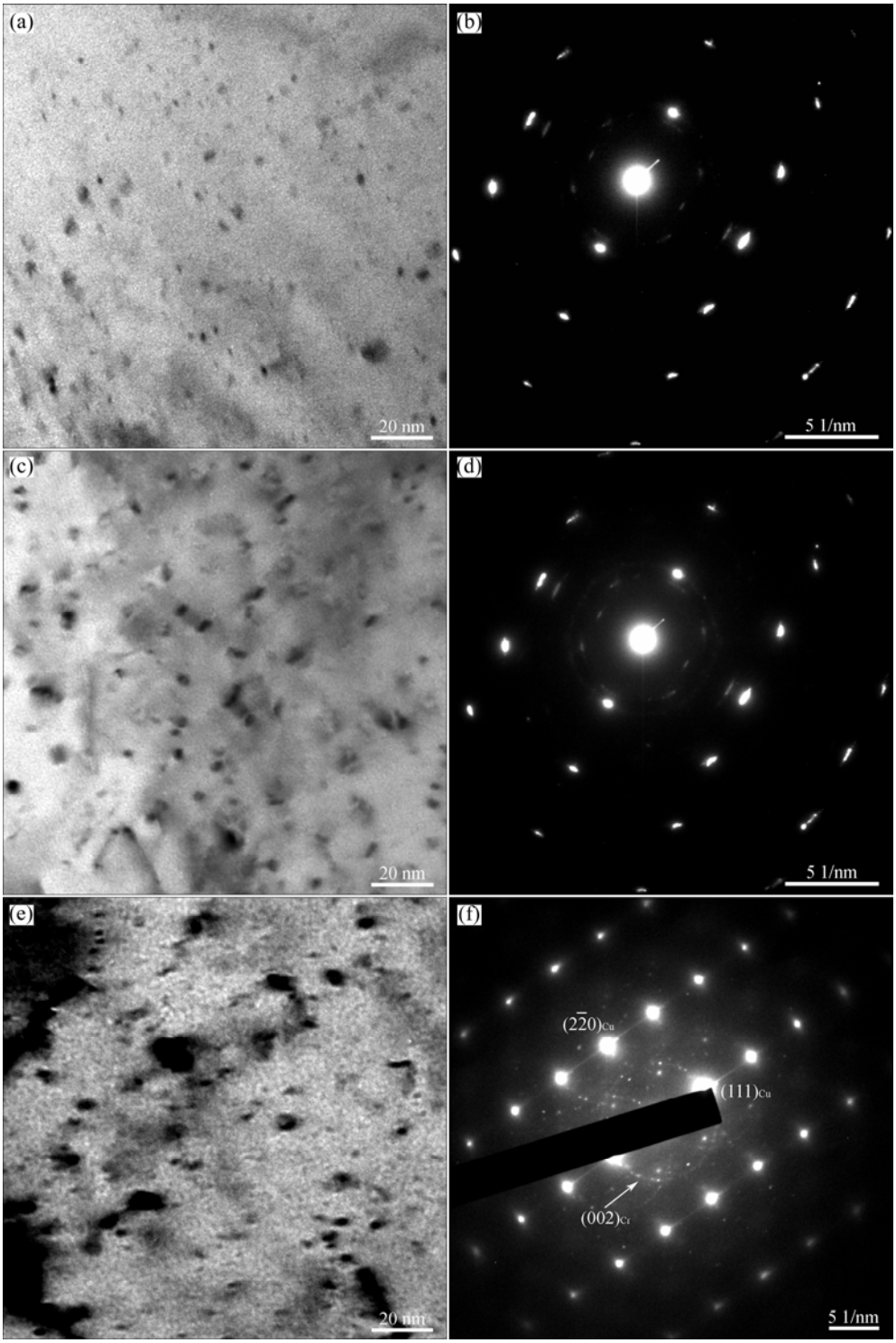

Fig. 9 Bright field TEM micrographs and SAED patterns of specimens cold rolled up to 60% strain and aged at 723 K for 60 min (a, b), 773 K for 60 min (c, d), and 823 K for 60 min (e, f)

effectively. As the aging temperature increases to 823 K, the position of the microhardness peak shifts to 30 min (Fig. 5(a)). Accompanied with a significant decrease of the microhardness, the specimen is overaged. In this case, the precipitates are coarsened by merging each other, bringing about a rapid rise in their size (Fig. 9(e)). Correspondingly, the gap between two adjacent precipitates becomes larger and the microhardness declines obviously.

The indexing result of the diffraction patterns in Figs. 9(b) and (d) is shown in Fig. 10. It is clear that the precipitates are the BCC Cr phase and FCC Cu_5Zr phase. Besides, there are no other reflection spots. The BCC Cr precipitates exhibit the well known Nishiyama−

Wassermann orientation relationship [20−22] with the Cu matrix: (111)Cu//(110)Cr, $[0\bar{1}1]$ Cu//[001]Cr, $[\bar{2}11]$ Cu// $[\bar{1}10]$ Cr. The close-packed planes of FCC (111) and BCC (110) are parallel in this two phases. At the overaging stage, diffraction rings characterizing no-coherent nano crystals with the Cu matrix appear beside the diffraction spots reflecting the Nishiyama−Wassermann orientation relationship between the precipitates and the matrix (Fig. 9(f)). This indicates that a sequential transition from coherent to semi-coherent to non-coherent relationship goes on with the aging. As a result, the microhardness decreases with increasing the aging time after reaching the microhardness peak or increasing the aging temperature above 773 K.

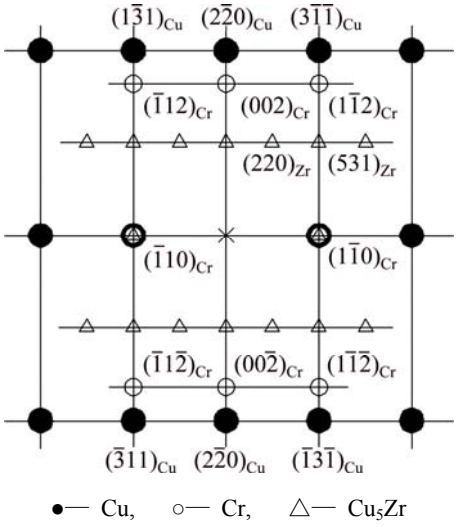

Fig. 10 Schematic drawing of SAED patterns in Figs. 9(b) and (d), showing coherent relationship between precipitated phases and matrix

4 Conclusions

1) Addition of Y and La to Cu−0.81Cr−0.12Zr alloy does not change the phase constitution. The alloy ingot and aged specimen are still composed of three phases: copper matrix, Cr and Cu_5Zr.

2) Compared with addition of only 0.5% La or 0.5% Y, the simultaneous addition of 0.5% La and 0.5% Y increases the microhardness to a higher level while the induced decrease in electrical conductivity is the lowest. The best comprehensive property of Cu−0.81Cr−0.12Zr−0.05La−0.05Y alloy is obtained when it is aged at 773 K for 60 min. The microhardness reaches HV 186 while the electrical conductivity maintains at 81% IACS.

3) The crystal orientation of the rolled Cu−0.81Cr−0.12Zr−0.05La−0.05Y alloy gradually changes with the increasing aging temperature. The microstrain in the cold-rolled specimens is very high due to the interaction of precipitations and dislocations.

4) The precipitates in the aged sample are the BCC Cr phase and FCC Cu_5Zr phase, which exhibit the N−W orientation relationship with the matrix before overaging takes place. Coherence strengthening mechanism should be responsible for the rise of microhardness at the peak position.

References

[1] CHIHIRO W, RYOICHI M, KAZUE T. Mechanical properties of Cu−Cr system alloys with and without Zr and Ag [J]. J Mater Sci, 2008, 43: 813−819.

[2] ZENG K J, HAMMALAINEN H. A theoretical study of the phase equilibrium in the Cu−Cr−Zr alloy [J]. J Alloys Compd, 1995, 220: 53−61.

[3] KALININ G, MATERA R. Comparative analysis of copper alloys for the heat sink of plasma facing components in ITER [J]. J Nucl Mater, 1998, 258−263: 345−350.

[4] SU J H, LIU P, DONG Q M, LI H J. Microstructure and properties of Cu−Cr−Zr alloy after rapidly solidified aging and solid solution aging [J]. J Mater Sci Technol, 2005, 21: 475−478.

[5] SU J H, LIU P, DONG Q M, LI H J, REN F Z. Aging study of rapidly solidified and solid-solution Cu−Cr−Sn−Zn alloy [J]. J Mater Process Technol, 2008, 205: 366−369.

[6] MU S G, GUO F A, TANG Y Q, CAO X M, TANG M T. Study on microstructure and properties of aged Cu−Cr−Zr−Mg−RE alloy [J]. Mater Sci Eng A, 2008, 475: 235−240.

[7] XIE M, LIU J L, LU X Y, SHI A, DEN Z G, JANG H, ZHENG F Q. Investigation on the Cu−Cr−RE alloys by rapid solidification [J]. Mater Sci Eng A, 2001, 304−306: 529−533.

[8] TSENG A A, LIN F H, GUNDERIA A S, NI D S. Roll cooling and its relationship to roll life [J]. Metall Trans A, 1989, 20: 2305−2320.

[9] PAN Z Y, CHEN J B, ZHOU W, LI J F. Microstructure and properties of rapidly solidified Cu−0.81Cr−0.12Zr alloy [J]. Mater Trans, 2013, 54: 1403−1407.

[10] TENWICK M J, DAVIES H A. Enhanced strength in high conductivity copper alloys [J]. Mater Sci Eng A, 1988, 98: 543−546.

[11] CHINH N Q, GUBICZA J, LANGDON T G. Characteristics of face-centered cubic metals processed by equal-channel angular pressing [J]. J Mater Sci, 2007, 42: 1594−1605.

[12] TSUCHIYA K, KAWAMURA H. Mechanical properties of Cu−Cr−Zr alloy and SS316 joints fabricated by friction welding method [J]. J Nucl Mater, 1996, 233−237: 913−917.

[13] FANG Jun-xing, CHEN Dong. Introduction to solid state physics [M]. Beijing: High Education Press, 1981. (in Chinese)

[14] LOTGERING F K. Topotactical reactions with ferromagnetic oxides having hexagonal crystal structures—I [J]. J Inorg Nucl Chem, 1959, 9: 113−123.

[15] ZHANG Y, TAO N R, LU K. Mechanical properties and rolling behaviors of nano-grained copper with embedded nano-twin bundles [J]. Acta Mater, 2008, 56: 2429−2440.

[16] QIAN L H, WANG S C, ZHAO Y H, LU K. Microstrain effect on thermal properties of nanocrystalline Cu [J]. Acta Mater, 2002, 50: 3425−3434.

[17] TORRE F D, LAPOVOK R, SANDLIN J, THOMSON P E, DAVIES C H J, PERELOMA E V. Microstructures and properties of copper processed by equal channel angular extrusion for 1–16 passes [J]. Acta Mater, 2004, 52: 4819−4832.

[18] HONG S I, HILL M A. Mechanical stability and electrical conductivity of Cu−Ag filamentary microcomposites [J]. Mater Sci Eng A, 1999, 264: 151−158.

[19] LIM M S, SONG J S, HONG S I. Microstructural and mechanical stability of Cu−6wt.%Ag alloy [J]. J Mater Sci, 2000, 35: 4557−4561.

[20] CHIBIHI A, SAUVAGE X, BLAVETTE D. Atomic scale investigation of Cr precipitation in copper [J]. Acta Mater, 2012, 60: 4575−4585.
[21] FUJII T, NAKAZAWA H, KATO M, DAHMEN U. Crystallography and morphology of nanosized Cr particles in a Cu−0.2% Cr alloy [J]. Acta Mater, 2000, 48: 1033−1045.
[22] BATRA I S, DEY J K, KULKARNI U D, BANERGEE S. Microstructure and properties of a Cu−Cr−Zr alloy [J]. J Nucl Mater, 2001, 299: 91−100.

含稀土 Cu−Cr−Zr 合金的微观组织和性能

潘振亚，陈讲彪，李金富

上海交通大学 材料科学与工程学院 金属基复合材料国家重点实验室，上海 200240

摘 要：先后热轧、固溶处理、冷轧和时效处理 Cu−0.81Cr−0.12Zr−0.05La−0.05Y(质量分数)合金，并系统研究其不同阶段的微观结构、显微硬度和导电率的变化规律。合金铸态组织由 Cu 基体、Cr 相和 Cu_5Zr 三相组成。经固溶处理后，Zr 相充分溶于 Cu 基体中，而部分 Cr 相仍残留于 Cu 基体中。样品冷轧后的时效处理使 Cr 与 Cu_5Zr 纳米析出相从基体中析出，且基体显微硬度和导电率增加。在 773 K 时效 60 min 后，样品获得了高显微硬度(HV 186)和高导电率(81% IACS)。随着时效温度的提高，Cu 晶体的取向度逐渐减小到零，而微应变因存在析出相和位错的相互作用未能得到完全的释放。当共格强化机制在合金中起主要增强作用时，Cr 析出相与铜基体之间保持着 N−W 的位相关系。

关键词：Cu−Cr−Zr−RE 合金；轧制；时效处理；微观结构；性能

(Edited by Xiang-qun LI)